Nanoaggregates and Structure–Function Relations in Asphaltenes†

8 **AUTHORS**, INCLUDING:

Gaëlle Andreatta
Centre Suisse d'Electronique et de Microtech…
11 PUBLICATIONS   314 CITATIONS

SEE PROFILE

Elías Pérez
Universidad Autónoma de San Luis Potosí
79 PUBLICATIONS   546 CITATIONS

SEE PROFILE

Oliver C Mullins
Schlumberger Limited
244 PUBLICATIONS   5,938 CITATIONS

SEE PROFILE

Nanoaggregates and Structure−Function Relations in Asphaltenes[†]

Gaelle Andreatta,[‡] Cristiane Carla Goncalves,[‡,§] Gabriel Buffin,[‡] Neil Bostrom,[‡] Cristina M. Quintella,[‡] Fabricio Arteaga-Larios,[#] Elías Pérez,[#] and Oliver C. Mullins*,[‡]

Schlumberger−Doll Research, Old Quarry Road, Ridgefield, Connecticut 06877, Instituto de Química, Universidade Federal da Bahia, Campus de Ondina, 40.170-290, Brazil, and Instituto de Fisica, Universidad Autonoma de San Luis Potosi, Alvaro Obregon 64, 78000 SLP, Mexico

The goal of predictive science is to establish structure−function relations for a system of interest. The obvious first step is to determine the structure of the system. Predictions in asphaltene science have been greatly inhibited, because of disagreement regarding molecular weight and molecular structure. With substantial progress on both structural fronts, structure−function relationships can be explored. Here, high quality factor (high-Q) ultrasonics is used to demonstrate asphaltene nanoaggregation at ∼100 mg/L. Fluorescence quenching measurements corroborate these results. Simple concepts regarding asphaltene molecular structure can be used to understand asphaltene nanoaggregation. These relations are seen to apply for asphaltene samples of very different origin. The implications of this understanding on larger-scale asphaltene aggregation and solubility are discussed.

I. Introduction

"If you want to understand function, study structure", advises Francis Crick.[1] This sage advice places a premium on proper structural information. Without structural information, predictive science is generally precluded and phenomenology prevails. The application of proper predictive science for crude oils and asphaltenes is embodied in the name of a new field: petroleomics. Consequently, the success of petroleomics hinges on the basic structural determination of crude oils, including (and especially) asphaltenes. The functional or operational issues of asphaltenes, which are the most aromatic component of crude oil, are of enormous importance in the production, transportation, and refining of crude oil as well as in paving and coating materials.[2−5] However, the uncertainties associated with asphaltene molecular structure, coupled with the much larger length scales of concern for economic impact, have combined to preclude elucidation of structure−function relations. That is, disagreement of one or more orders of magnitude has surrounded determination of the molecular weight of asphaltenes. The distribution of asphaltene fused-ring systems is also of concern. In addition, the issues of operational concern associated with asphaltenes include flocculation and the rheology and interfacial activity of asphaltenic materials.[2−5] Uncertainties regarding proper asphaltene molecular structures, coupled with uncertainties of how these structures, if known, would impact larger length scale properties, has impeded Crick's axiom from being followed.

Asphaltene Molecular Weight. Recent advances in asphaltene molecular structure determination have improved the prospects establishing structure−function relations. In the early 1980s, Boduszynski determined that asphaltenes have a mean molecular mass of ∼700 g/mol with a factor of 2 in the width of their distribution.[6] However, these data were in direct contradiction to the interpretation of the vapor pressure osmometry (VPO) data. For an asphaltene sample, VPO will yield a weight that is dependent on solvent identity, temperature, and concentration.[7] Clearly, an aggregate weight is being measured, not the "molecular weight". The extent of asphaltene aggregation is dependent on solvent identity, temperature, and concentration. Extrapolation of VPO data at high concentration to zero concentration is uncertain, particularly because as-

[†] Presented at the 5th International Conference on Petroleum Phase Behavior and Fouling.

* Author to whom correspondence should be addressed. Telephone: 203 431 5572. Fax: 203 438 3819. E-mail address: omullins@ridgefield.oilfield.slb.com.

[‡] Schlumberger−Doll Research.

[§] Instituto de Química, Universidade Federal da Bahia.

[#] Instituto de Fisica, Universidad Autonoma de San Luis Potosi.

(1) Crick, F. *Phys. Today* **2000**, *53* (March), 19.

(2) Chilingarian, G. V., Yen, T. F., Eds. *Bitumens, Asphalts and Tar Sands*; Elsevier Scientific Publishing Co.: New York, 1978.

(3) Bunger, J. W., Li, N. C., Eds. *Chemistry of Asphaltenes*; Advances in Chemistry Series, 195; American Chemical Society: Washington, DC, 1981.

(4) Sheu, E. Y., Mullins, O. C., Eds. *Asphaltenes: Fundamentals and Applications*; Plenum Press: New York, 1995.

(5) Mullins, O. C., Sheu, E. Y., Eds. *Structure and Dynamics of Asphaltenes*; Plenum Press: New York, 1998.

(6) Boduszynski, M. M. In *Chemistry of Asphaltenes*; Bunger, J. W., Li, N. C., Eds.; Advances in Chemistry Series, 195; American Chemical Society: Washington, DC, 1981; Chapter 7.

(7) Weihe, I.; Liang, K. S. *Fluid Phase Equilib.* **1996**, *117*, 201.

phaltenes are likely to have a hierarchy of aggregation. That is, tightly bound nanoaggregates might not be amenable to dissociation at high concentration, whereas clusters of nanoaggregates can be efficiently dissociated. Thus, extrapolation limits from high concentration do not necessarily imply molecular dispersions.

This unfortunate situation behooves resolution. In a series of papers, we have shown that time-resolved fluorescence depolarization (FD) techniques can be used to determine the rotational diffusion constants of asphaltenes in dilute solution (typically 10 mg/L or less).[8−13] The FD results conclude that virgin crude oil asphaltenes have a mean molecular weight of ∼750 g/mol with a factor of 2 width. These publications report results in close agreement with Boduszynski's early work in field ionization mass spectroscopy (FIMS).[6] Many different types of asphaltenes are used in these studies, from many virgin crude oils, hydrocracked samples, asphaltene solubility subfractions, coal and bitumen. These FD results are general and are not specific to a particular asphaltene. The FD results probe molecular size. Direct imaging measurements of scanning tunneling microscopy (STM), which images the aromatic portion of the molecule, are consistent with size limits placed by the FD studies.[14] The imaging of petroleum asphaltenes by high-resolution transmission electron microscopy (HRTEM) also provides consistent measurements of aromatic ring sizes both for petroleum and for the smaller coal asphaltenes.[15] In addition, a variety of mass spectral studies have confirmed this range of asphaltene molecular weights. Some, but not all, studies that use laser desorption mass spectroscopy (LDMS) or matrix-assisted laser desorption ionization (MALDI) mass spectroscopy have arrived at similar asphaltene molecular weights.[16−18] Atmospheric-pressure chemical ionization (APCI) mass spectroscopy[19] and atmospheric-pressure photoionization ionization (APPI) mass spectroscopy[20] also find consistent results. It is important to note that some laser desorption studies yield much-larger results for similar carbonaceous samples.[21] Laser desorption methods do have significant baseline issues. The highest-resolution and

highest-mass-accuracy mass spectrometer ever used on carbonaceous materials gets consistent results on upper limits for asphaltene molecular weight using heavy Venezuelan crude oils, among other samples.[22,23] Here, the ionization method is the very soft electrospray ionization (ESI) on a Fourier transform ion cyclotron mass spectrometry (FT-ICR-MS) system. A consensus is building from many different techniques regarding the molecular weight of asphaltenes.

The FD results also indicate that most asphaltene molecules possess one or perhaps two aromatic ring systems per molecule.[8−13] Small asphaltene chromophores undergo rotational random walk up to 10 times faster than large asphaltene chromophores. Furthermore, the small asphaltene chromophores undergo rotational diffusion at the same rate as octaethyl porphyrin (OEP). The FD results on OEP are in agreement with results obtained previously on OEP by a perturbed angular correlation of γ-rays.[24] The small asphaltene chromophores are not tethered to large groups, which would restrict the rotation degrees of freedom. The average number of fused rings in petroleum aromatic molecules has been reported to be 4−10 rings by a variety of measurements. These values are consistent with direct molecular imaging of asphaltene molecules via STM[14] and HRTEM.[15] FD results are consistent with this determiantion.[8,13]

Fused-Ring Geometry. Another important molecular structural issue is the configuration of the fused rings. Multiple aromatic rings can be shared at two verticies (catacondensed) or three verticies (pericondensed). Carbon X-ray Raman spectral (XRRS) studies show that asphaltene ring systems are pericondensed, as determined by comparing asphaltenes with a large number of polycyclic aromatic hydrocarbons.[25] Generally, pericondensation is known to yield more stable structures.[26] It is not surprising to find the requirement of energy stability for asphaltenes derived from carbonaceous materials in place for geologic time. The experimental XRRS measurements have been corroborated by calculated predictions of X-ray Raman spectra.[27] Also note that the optical properties of asphaltenes mandate that the predominant ring systems are not small: small pericyclic (e.g., perylene, pyrene, etc.) ring systems are colorless, whereas asphaltenes are not colorless.[26]

The molecular structure emerges such that asphaltene molecules are shaped "like your hand", with an aromatic core (palm) with associated alicyclic rings, and with alkyl groups hanging off the periphery (fingers). One immediately concludes that competing intermolecular interactions are dominate for asphaltenes; van der Waals binding via stacking of aromatic ring systems vs steric repulsion associated with alkane

(8) Groenzin, H.; Mullins, O. C. *J. Phys. Chem. A* **1999**, *103*, 11237.

(9) Groenzin, H.; Mullins, O. C. *Energy Fuels* **2000**, *14*, 677.

(10) Buenrostro-Gonzalez, E.; Groenzin, H.; Lira-Galeana, C.; Mullins, O. C. *Energy Fuels* **2001**, *15*, 972.

(11) Groenzin, H.; Mullins, O. C.; Eser, S.; Mathews, J.; Yang, M.-G.; Jones, D.; *Energy Fuels* **2003**, *17*, 498.

(12) Buch, L.; Groenzin, H.; Buenrostro-Gonzalez, E.; Andersen, S. I.; Lira-Galeana, C.; Mullins, O. C. *Fuel* **2003**, *82*, 1075.

(13) Badre, S.; Goncalves, C. C.; Mullins, O. C. Submitted to *Fuel*.

(14) Zajac, G. W.; Sethi, N. K.; Joseph, J. T. *Scanning Microsc.* **1994**, *8*, 463.

(15) Sharma, A.; Groenzin, H.; Tomita, A.; Mullins, O. C. *Energy Fuels* **2002**, *16*, 490.

(16) Miller, J. T.; Fisher, R. B.; Thiyagarajan, P.; Winans, R. E.; Hunt, J. E. *Energy Fuels* **1998**, *12*, 1290.

(17) Yang, M.-G.; Eser, S. *Prepr. Symp.—Am. Chem. Soc., Div. Fuel Chem.* **1999**, *44*, 768. (Preprints of the 218th ACS National Meeting, New Orleans, LA, 1999.)

(18) Mochida, I.; Kinoshita, Y.; Kuramae, M.; Choi, K.-H.; Korai, Y. Unexpected Problems Caused by Dry Sludge in the Upgrading Processes of Petroleum Products. Presented at the 5th International Conference on Petroleum Phase Behavior and Fouling (Banff Conference on Heavy Oil), June 13−17, 2004, Paper No. 33.

(19) Cunico, R. I.; Sheu, E. Y.; Mullins, O. C. *Pet. Sci. Technol.* **2004**, *22* (7&8), 787−798.

(20) Desmazières, B.; Merdrignac, I.; Laprévote, O.; Terrier, P. Analysis of Oil Asphaltenes by SEC and SEC-MS Coupling. Presented at the 5th International Conference on Petroleum Phase Behavior and Fouling (Banff Conference on Heavy Oil), June 13−17, 2004, Paper No. 104.

(21) Suelvas, I.; Islas, C. A.; Millan, M.; Galmes, C.; Carter, J. F.; Herod, A. A.; Kandiyoti, R. *Fuel* **2003**, *82*, 1.

(22) Qian, K.; Rodgers, R. P.; Hendrickson, C. L.; Emmett, M. R.; Marshall, A. G. *Energy Fuels* **2001**, *15*, 492.

(23) Hughey, C. A.; Rodgers, R. P.; Marshall, A. G. *Anal. Chem.* **2002**, *74*, 4145.

(24) Mullins, O. C.; Kaplan, M. *J. Chem. Phys.* **1983**, *79*, 4475.

(25) Bergmann, U.; Groenzin, H.; Mullins, O. C.; Glatzel, P.; Fetzer, J.; Cramer, S. P. *Chem. Phys. Lett.* **2003**, *369*, 184.

(26) Ruiz-Morales, Y. *J. Chem. Phys. A* **2002**, *106*, 11283.

(27) Gordon, M. L.; Tulumello, D.; Cooper, G.; Hitchcock, A. P.; Glatzel, P.; Mullins, O. C.; Cramer, S. P.; Bergmann, U. *J. Phys. Chem. A* **2003**, *107*, 8512.

chains. These standard chemical interactions are utilized by the dye industry: to make an aromatic dye more soluble, alkane substituents often are added. The increased steric repulsion can dramatically increase solubility. A comparison of coal versus crude oil asphaltenes proves this expectation. Coals are much more aromatic and have a much less alkane fraction than petroleum. Thus, asphaltenes derived from coals also possess much smaller alkane fractions than petroleum asphaltenes.[10] Thus, coal asphaltnees are subject to much less steric repulsion than petroleum asphaltenes. Consequently, to maintain the same solubility (the definition of asphaltene), coal asphaltenes must have lesser van der Waals attraction to maintain the balance of intermolecular attractive and repulsive forces. Therefore, coal asphaltenes must possess smaller fused-ring systems. This has been shown by fluorescence emission and FD measurements,[10,13] as well as through direct molecular imaging of coal and petroleum asphaltenes.[15] This important result relates molecular structure with function—in this case, solubility.

There is a complication relating molecular structure with solubility. There are potentially different stages of aggregation in asphaltenes, for instance, as proposed in the Yen model. The question arises as to the role of possible hierarchical aggregation structures of asphaltenes and solubility. Recent data have suggested that asphaltenes in toluene form nanoaggregates. Laser thermal lensing in asphaltene solutions shows an extremum at ~60 mg/L.[28] Recent fluorescence measurements of the intensity and red shift indicate that asphaltenes aggregate at 60 mg/L in toluene.[29] These results are suggestive of a change in aggregation but are not directly interpretable in terms of physical parameters. High-quality-factor (high-*Q*) ultrasonic spectroscopy clearly shows asphaltene aggregation at ~100 mg/L.[30] In addition, new conductivity measurements of asphaltene solutions also clearly exhibit ashaltene aggregation at ~120 mg/L.[31]

Recent high-resolution, high-*Q* ultrasonics spectroscopy results clearly show an abrupt change in the speed of sound of asphaltene−toluene solutions at ~100 mg/L.[30] In that work, critical micelle concentrations (CMCs) of various surfactants are reported, proving the reliability of this method for detection of aggregation. In particular, the measurement of CMCs of three standard surfactants in water were demonstrated: sodium dodecyl sulfate (SDS) at 2.59 g/L, cetyl trimethyl ammonium bromide (C_{16}TAB) at 0.338 g/L, and Tween 80 at 0.008 g/L, all of which are quite similar to the reported literature values. In addition, our values of compressibilities, which have been derived from ultrasonic velocity and density measurements, are all quite similar to literature values for both monomers and micelles.[30] Thus, high-*Q* ultrasonics works over a broad range of concentrations. In the middle of this range— that is, in the sweet spot of the ultrasonics method— the asphaltenes exhibited aggregation. There are many reasons to believe that the aggregation numbers are

small; thus, we refer to these as nanoaggregates. In particular, the molecular weights reported by VPO are often a factor of ~5 too high in the concentration range where the ultrasonics,[30] fluorescence,[29] thermal lensing,[28] and conductivity[31] all show asphaltene aggregation. Thus, we consider the aggregation number to be on the order of 5. Many argue that "micelle" is the term that is preferred to be used for the one phase that is separated from a second phase by a surfactant. Thus, we use the terms "nanoaggregate" and "critical nanoaggregate concentration" (CNAC), not micelle, to describe the asphaltene aggregation phenomenon.[32] However, we note that there is abundant literature that claims to have measured the asphaltene CMC. Typical concentrations are reported to be several grams per liter. Our work and others cited herein show that the CNAC at 100 mg/L is in direct contradiction to reports of the asphaltene CMC at several grams per liter. The modified terminology should not confuse this point. This potential confusion makes us somewhat reluctant to change the terminology.

In this report, new high-*Q* ultrasonic results are presented, confirming that asphaltenes undergo aggregation at ~100 mg/L. Relative fluorescence quantum yield measurements corroborate these results. In addition, the ultrasonics data imply that asphaltene nanoaggregates have a maximum size limit. Very different source materials are used to explore asphaltene aggregation versus molecular structure relations. Structure−function relations are proposed that control asphaltene stability, with regard to flocculation in toluene solutions. The importance of polydispersity is suggested, and the relation of these findings to crude oils is suggested.

II. Experimental Section

N-heptane asphaltenes and maltenes from UG8 Kuwaiti crude oil were used; the extraction procedure is described elsewhere.[8] The organic solutions were prepared in toluene (99.8%, from Acros and Sigma−Aldrich).

The ultrasonic measurements were performed on a high-resolution ultrasonic spectrometer (model HRUS 102, from Ultrasonic Scientific, Ltd.).[33] The speed of sound was determined using the resonance technique in the frequency range of 2−20 MHz. We used a frequency of ~5 MHz for our experiments; the spectrometer can measure the speed of sound to 1 part in 4×10^{-6}. The measurements were made using two identical cells filled with a volume of 1−2 mL: one was filled with the analyte solution, and the other was filled with the solvent (toluene). Both cells were fixed together in the same block and were thermostated at 25.0 ± 0.1 °C, enabling small differences in ultrasonic velocity to be determined.[30,33] Each cell consisted of a resonance cavity with a resonant glass chamber built in, with two lithium niobate transducers on two opposite sides of the cell; one transducer was used as the signal source, and the other was the receiver.[33] Two main factors determine the resolution of the measurements: the quality of the resonance (including a high *Q* and the absence of satellites of the resonance peaks) and the stability of the resonances. The first factor is ensured by having a high precision in the parallel alignment of the cells and the quality of the lithium niobate piezotransducers. The second factor requires special construction of the resonator, insisting on keeping the distance

(28) Acevedo, S.; Ranaudo, M. A.; Pereira, J. C.; Castillo, J.; Fernandez, A.; Perez, P.; Caetano, M. *Fuel* **1999**, *78*, 997.
(29) Goncalves, S.; Castillo, J.; Fernandez, A.; Hung, J. *Fuel* **2004**, *83*, 1823.
(30) Andreatta, G.; Bostrom, N.; Mullins, O. C. *Langmuir*, in press.
(31) Sheu, E. Y. Manuscript in preparation.

(32) We thank Professor Johan Sjoblom for suggesting this terminology.
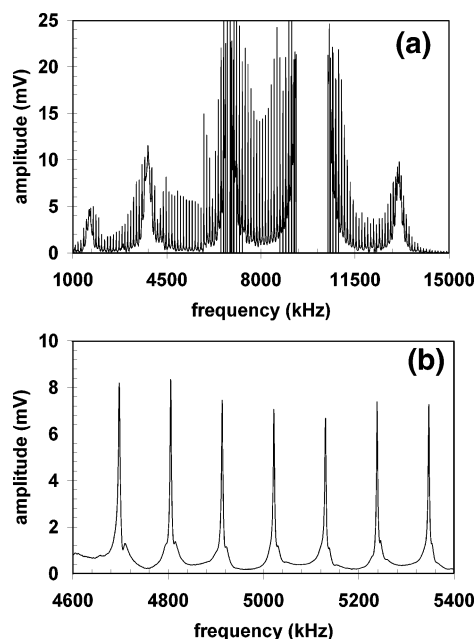(33) Buckin, V.; Smyth, C. *Semin. Food Anal.* **1999**, *4* (2), 113−130.

Figure 1. (a) High-quality-factor (high-Q) ultrasonic spectrum of toluene at 25 °C. The narrow cavity resonances can be used to accurately measure spectral properties. (b) Ultrasonic cavity resonances at 5 MHz of toluene on an expanded scale. Subtle shifts in peak positions versus analyte concentration can be recorded, giving a very accurate speed of sound.

between the two transducers constant. To maintain a perfect geometry, the resonator chamber has been built separately from the transducers. Of course, frequencies can be measured to very high accuracies. The conversion of frequency to sound speed is performed using the equation

$$\frac{\delta u}{u} = \frac{\delta f_n}{f_n} \qquad (1)$$

where u is the speed of sound and f_n is the frequency of the nth resonance. This equation presumes plane wave propagation in an ideal one-dimensional resonator.[34] A typical ultrasonic spectrum of toluene is shown in Figure 1a. Several of the sharp ultrasonic resonances are shown in Figure 1b at the frequency range used for this study. In these figures, the amplitude of the output signal is shown as a function of the frequency of the acoustical signal. In addition to the narrow acoustic cell resonances, Figure 1a shows broad resonances (at ~4, 7, and 10 MHz, for example) that are associated with ultrasonic resonances in the glass walls of the cells and with the transducers. These spectral regions were avoided in all of our experiments. In toluene, at 25 °C, the speed of sound has been measured to be $u_0 = 1307.1$ m/s, with a resolution of 0.0052 m/s.

All ultrasonic spectra were acquired by diluting solutions from the highest concentrations, with stepwise concentration reductions. Each curve consisted of approximately 15 to 25 points. For each point, a quantitative dilution was performed; the solution was stirred and allowed to equilibrate for 15−20 min prior to recording the ultrasonic frequency for that concentration. Integrated runs were typically 4−6 h. No difference in the spectrum was observed if the equilibration time was increased or decreased by a factor of 2. The reproducibility of the measurements was examined and determined to be very good. All the ultrasonic titrations exhibit a break between two segments in the curves. The higher-concentration

(34) Bolef, D. I.; Miller, J. G. High- Frequency Continuous Wave Ultrasonics (Chapter 3). In *Physical Acoustics*, Vol. VIII; Mason, W. P., Thurston, R. N., Eds.; Academic Press: New York, 1971.
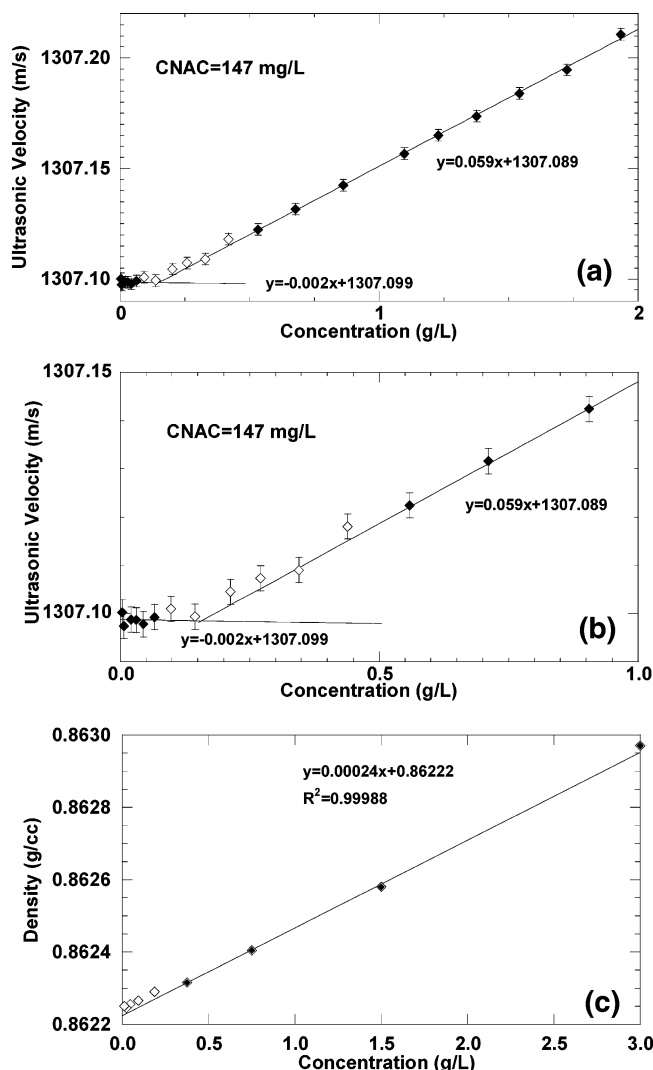
side is clearly straight. At concentrations below the break, the points were fit to a straight line, to obtain the CNAC. There may be some structure to this region; however, our current sensitivity is insufficient to measure this accurately.

The fluorescence measurements were performed with a PTI model A-720 steady-state fluorescence spectrometer. A 1-mm cuvette was used to keep path lengths to a minimum, so that self-absorption effects are reduced. Comparison was made between absorption strength (determined with a Cary 5 UV−visible−NIR spectrometer) and the fluorescence intensity of relevant solutions, thereby giving a relative quantum yield. The asphaltenes were dissolved in toluene, whereas the dye was dissolved in methanol.

III. Theory

The ultrasonic data can be analyzed in terms of the phase equilibrium model, which has originally been developed for micellization (see ref 30 and references therein). In particular, we use this phase-equilibrium micelle formalism for asphaltenes, because the asphaltene nanoaggregates produce an ultrasonic curve with a constant slope above the CNAC. That is, the asphaltene nanoaggregates seem to have a maximum size limit. This is contrasted by other nonionic surfactants in toluene, as will be shown. These nanoaggregates can thus be treated as entities with a reasonably well-defined density and, more importantly, compressibility. The phase-equilibrium model presumes that the monomer concentration remains unchanged above the CNAC; we assume this is correct for asphaltenes.

The speed of sound is given by

$$u = \frac{1}{\sqrt{\rho \kappa}} \qquad (2)$$

If we assume that the phase-equilibrium model for micellization is valid here, then

$$c_1 = c \text{ and } c_{NA} = 0 \qquad (\text{for } c < \text{CNAC})$$

$$c_1 = \text{cnac and } c_{NA} = c - \text{cnac} \qquad (\text{for } c > \text{CNAC})$$

where c is the weight concentration of the solution, cnac is the numerical value of the concentration at the CNAC, and c_{NA} is the concentration of nanoaggregates.

For dilute solutions:

$$\rho = \rho_0 + (1 - \tilde{v}_1 \rho_0)c \qquad (\text{for } c < \text{cnac}) \qquad (3)$$

$$\rho = \rho_0 + (\tilde{v}_m - \tilde{v}_1)\rho_0 \text{cnac} + (1 - \tilde{v}_m \rho_0)c$$
$$(\text{for } c > \text{cnac}) \quad (4)$$

where v_0 is the specific volume of the solvent ($v_0 = 1/\rho_0$), $\tilde{v}_1$ the apparent specific volume of the monomeric form, and $\tilde{v}_m$ the apparent specific volume of the nanoaggregate form. The tilde represents apparent parameters; that is, a change in the solution parameter v with a specific increment of solute 1 is denoted as $\tilde{v}_1$.

With similar considerations for the compressibility, one obtains the relation given in eq 5 for the speed of sound:[30]

$$u = u_0 + \frac{u_0}{2}\left[\tilde{v}_1\left(2 - \frac{\tilde{\kappa}_1}{\kappa_0}\right) - \tilde{v}_{NA}\left(2 - \frac{\tilde{\kappa}_{NA}}{\kappa_0}\right)\right]\text{cnac} +$$
$$\frac{u_0}{2}\left[\tilde{v}_{NA}\left(2 - \frac{\tilde{\kappa}_{NA}}{\kappa_0}\right) - v_0\right]c \quad (5)$$

Figure 2. (a) Ultrasonic velocity of UG8 asphaltene in toluene versus concentration at 25 °C. The CNAC is evident as the break in the curve at 147 mg/L. (b) Expanded region of panel a for UG8 asphaltene in toluene around the CNAC concentration (147 mg/L). (c) Solution density of UG8 asphaltene in toluene at 25 °C.

κ corresponds to the compressibility, and the subscripts 0, 1, and NA represent the solvent, the asphaltene monomer, and the asphaltene nanoaggregates, respectively. At concentrations higher than CNAC, one obtains a straight-line prediction for the speed of sound with concentration, provided there is a single compressibility and density for the nanoaggregates.

IV. Results

Figure 2a shows the ultrasonic velocity curve for UG8 asphaltenes in toluene. Above the CNAC (the break point), the ultrasonic velocity is linearly dependent on concentration, with a very high degree of precision. Figure 2b expands the region near the CNAC to illustrate the validity of the measurement. (The open points in Figure 2a and 2b were not used to fit the straight-line sections displayed in the figure.) Below the CNAC, there is largely linear behavior but there is also a suggestion of perhaps more-complex behavior. It is difficult to say if this fine structure below CNAC is real, because it is smaller than the error. This ultrasonic data
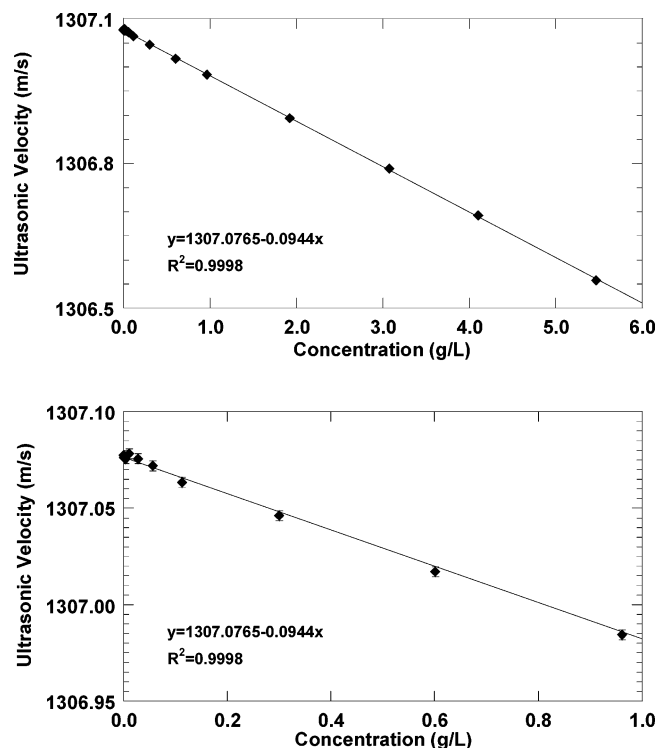
Figure 3. (a) Ultrasonic velocity of UG8 maltene in toluene. No break point is evident in this spectrum, and no aggregation is detected. (b) Expanded region of panel a for UG8 maltene in toluene at low concentration, showing that no break point is detected.

do not address possible dimer and trimer formation below CNAC. Figure 2c shows the density curve for UG8 asphaltene in toluene. The break at CNAC is not evident in the density data. Density is an integral quantity, whereas compressibility is a differential quantity. Consequently, compressibility and, thus, ultrasonic velocity (eq 2) are much more sensitive to subtle changes than is density. Using the measured ultrasonic changes and measured density changes above CNAC with eq 5, one obtains, for the nanoaggregates, the apparent specific volume—$\tilde{v}_{NA} = 0.8814$ cm^3/g—and the apparent adiabatic compressibility—$\tilde{k}_{NA} = 3.95 \times 10^{-5}$/bar.[30] This compressibility is known to be comparable to those of other nonionic surfactant aggregates in toluene.[30] We do not list the comparable values for the monomers, because our density measurements did not have sufficient resolution at these low concentrations.

This clear break in the asphaltene curve is contrary to the behavior of UG8 maltenes in toluene shown in Figure 3a and expanded in Figure 3b. It would be difficult to confuse the maltene behavior with the asphaltene behavior; the maltenes reduce the speed of sound in toluene solutions, thereby exhibiting opposite trends, in comparison to asphaltenes. In addition, maltenes do not exhibit even a hint of a break in the speed-of-sound curve. (UG8 is a 25 API oil.) Figures 2b and Figure 3b cover similar ranges, proving that the high-Q ultrasonic technique can detect the presence and absence of aggregation. To obtain a detailed understanding of why the ultrasonic slopes are different for maltenes and asphaltenes, we need accurate density data.

Figure 4a shows the same curve for the Iino coal asphaltene (we thank Professor Iino for this sample),
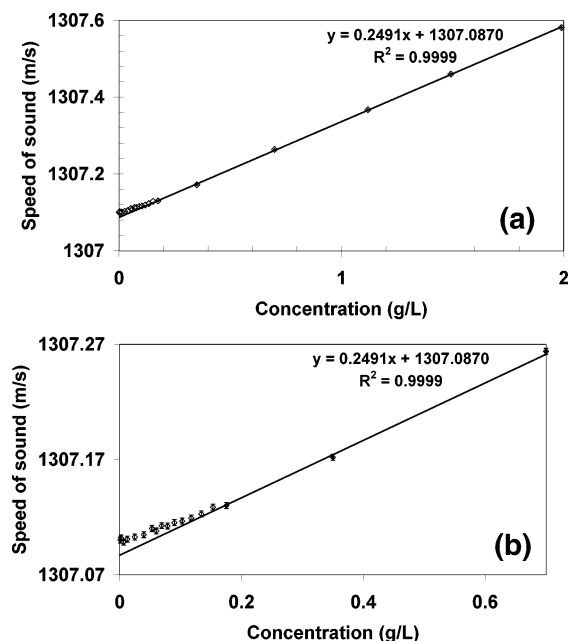
The impact of concentration-dependent micelle size on the ultrasonic curves is shown in Figure 6. Contrary to that observed in asphaltenes, there is no constant slope of the ultrasonic velocity curve above the aggregation threshold. That is, varying the size of the Brij35 aggregates at different concentrations produces varying compressibilities. With asphaltenes, the nanoaggregates exhibit a maximum size; increasing the concentration only increases the number of nanoaggregates. Thus, there is a well-defined compressibility of the asphaltene nanoaggregate and a single slope above CNAC. This size limit is consistent with small angle neutron scattering (SANS) data on asphaltenes.[39]

V. Discussion

A descriptive framework can be developed that accounts for, and is consistent with, a large body of work. First, asphaltene molecules are shaped "like your hand", with a single fused aromatic core and peripheral alicyclic and alkane substituents. A large fraction—if not most—of the heteroatom content resides in the aromatic core.[40] The asphaltene molecules associate strongly, by virtue of possessing large fused aromatic-ring systems. Certainly van der Waals attraction is very important here; however, there also will be some bonding due to charge separation associated with the heteroatoms, again largely in the aromatic core. Steric repulsion associated with the alkanes interferes with tight binding. The asphaltene solubility classification mandates a balance between the intermolecular binding, which is predominantly mediated via the aromatic core, and the steric hindrance induced by the alkyl carbon.[10] Asphaltenes with little alkane carbon (coal asphaltenes) exhibit little steric hindrance. To maintain the balance of intermolecular attraction and repulsion, these asphaltenes necessarily possess small fused ring systems. Therefore, asphaltenes with large alkyl carbon content (petroleum asphaltenes) possess large fused aromatic-ring systems. The solubility characteristics of these different asphaltene samples are, by definition, the same. In the solid state, these asphaltenes also exhibit the same stacking propensity and stacking geometry, even though the aromatic cores are of very different size.[15] Systematic variation of the asphaltene molecular structure accompanies hydrocracking of the feedstock.[12] These molecular considerations are broadly applicable.

Nanoaggregate formation of these samples occurs at fairly low concentrations, and the intermolecular binding energies are significant. The CNACs for very different asphaltenes are comparable, indicating that the balance between intermolecular attraction and repulsion is comparable, independent of the specific molecular structural features. Thus, coal asphaltene, with very little alkane carbon, and petroleum asphaltene, with >50% alkyl carbon, exhibit the same CNAC. The aggregation numbers of these aggregates are known to be rather low. The aggregate weights determined by VPO (and often incorrectly called molecular weights) are ∼5
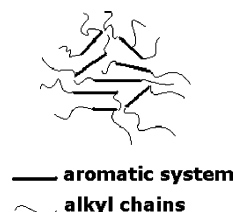

— aromatic system
∼ alkyl chains

Figure 7. Proposed schematic structure of asphaltene nanoaggregates. The rationale for this structure is consistent with a large body of work. Aggregates are likely not space-filling but, instead, are rather fluffy.

times larger than the asphaltene molecular weights.[8–13] We conclude that aggregate growth shuts off after the association of several molecules, because of excessive steric hindrance. That is, to achieve favorable interaction between two molecules, the alkane groups must be oriented to avoid interference with the other molecule. Subsequent association of each additional molecule in the aggregate constrains the alkyl groups further. However, steric hindrance is largely a local phenomenon. Thus, shutting off aggregate growth by steric hindrance mandates small aggregation numbers. Figure 7 schematically shows a proposed aggregate structure where there is favorable interaction of aromatic cores, but where steric hindrance prevents aggregate growth. This type of structure is consistent with direct molecular imaging of the solid state by HRTEM.[15] In particular, HRTEM shows very small stacks. Although HRTEM does suffer from edge effects, we believe that the "stack of pancakes" cannot get very large in asphaltene aggregates. The aggregate is likely not densely packed. This might explain how small aggregate numbers can be consistent with aggregates that have a physical radius on the order of 2.5 nm (and slightly larger radii of gyration).[39]

Polydispersity has a major role in asphaltene aggregation. The smaller asphaltene molecules can be viewed as being "chain terminators", whereas the larger asphaltene molecules are "chain propagators".[41] We use the words "large" and "small" a bit euphemistically here. By large molecules, we mean to indicate molecules that have more exposed aromatic core with less alkyl steric hindrance; this asphaltene fraction has lower solubility. By small molecule, we mean a molecule with less aromatic core exposed and with more alkane; this asphaltene fraction has greater solubility in toluene. It has been shown that these solubility fractions do correlate with molecular size;[11] however, the strengths of different intermolecular interactions are the true determinant here. If an asphaltene is separated into more-soluble and less-soluble fractions, then the less-soluble fraction has a much lower solubility in toluene.[42] We have seen this in our laboratory also. By removing the more-soluble fraction, one removes the chain terminators. Consequently, in solutions of the least-soluble fraction, only the chain propagators produced aggregates of large aggregation number, which gravity segregates. The polydispersity of a standard asphaltene sample naturally stabilizes nanoaggregates, which are suspended by Brownian motion. Increasing the concen-

(39) Sheu, E. Y.; Storm, D. A. In *Asphaltenes: Fundamentals and Applications*; Sheu, E. Y., Mullins, O. C., Eds.; Plenum Press: New York, 1995; Chapter 1.
(40) Mullins, O. C. In *Asphaltenes: Fundamentals and Applications*; Sheu, E. Y., Mullins, O. C., Eds.; Plenum Press: New York, 1995; Chapter 2.

(41) Agrawala, M.; Yarranton, H. W. *Ind. Eng. Chem. Res.* **2001**, *40*, 4664.
(42) Acevedo, S.; Escobar, O.; Echevarria, L.; Gutiérrez, L. B.; Méndez, B. *Energy Fuels* **2004**, *18*, 305.

tration of the asphaltene solution above CNAC simply increases the number of nanoaggregates, not their structure. At some much higher concentration, these nanoaggregates associate and eventually flocculate.

Note that trace water can have a role in the formation of nanoaggregates[43] and of nonionic surfactants in general. We have not determined the effect of trace water on asphaltene nanoaggregates here, nor have we tried to exclude trace water from our measurements. It would not be surprising to find that water might be very important. Natural crude oil systems have trace water; therefore, the results contained herein are likely related to crude oils in the natural state. Furthermore, the results herein are directly related to results from almost all results reported to date on nanoaggregates (or CMCs) in asphaltenes, because other laboratories also do not remove trace water in their asphaltene experiments.

VI. Conclusions

Nanoaggregation of asphaltene solutions at ~100 mg/L (±50%) is now established by high-Q ultrasonics and by fluorescence intensity measurements. These recent studies indicate that interfacial tension results purporting a critical micelle concentration (CMC) at ~2 g/L have been misinterpreted for the past decade. The growth and its termination of nanoaggregates can be understood directly from molecular structural considerations. The formation of nanoaggregates essentially consumes high-energy binding sites. The resulting nanoaggregates resembles a "hairy tennis ball", with alkanes surrounding the outside. These nanoaggregates are stable and do not grow; the absence of available high-energy binding sites prevents flocculation at moderate asphaltene concentrations. If the least-soluble fraction of asphaltenes is isolated, then aggregate growth proceeds unhindered, yielding low observed solubilities. The polydispersity in a standard asphaltene sample ensures nanoaggregate initiation from the least-soluble molecular fraction and nanoaggregate termination from the most-soluble molecular fraction, thereby creating a stable (nano)colloidal suspension. Because the crude oils are even more polydisperse, this implies that the same nanoaggregate formation and stabilization occurs in crude oils. In large measure, these results are in concert with the basic premise of the Yen model introduced so many years ago. This study fits within the ultimate goal of petroleomics—to relate detailed structural information of asphaltenes to their phenomenology.

EF0497762

(43) Andersen, S. I.; del Rio, J. M.; Khvostitchenko, D.; Shakir, S.; Lira-Galeana, C. *Langmuir* **2001**, *17*, 307.